Reducing Amygdala Activity and Phobic Fear through Cognitive Top–Down Regulation

Eva Loos*, Nathalie Schicktanz*, Matthias Fastenrath, David Coynel, Annette Milnik, Bernhard Fehlmann, Tobias Egli, Melanie Ehrler, Andreas Papassotiropoulos, and Dominique J.-F. de Quervain

Abstract

■ The amygdala is critically involved in emotional processing, including fear responses, and shows hyperactivity in anxiety disorders. Previous research in healthy participants has indicated that amygdala activity is down-regulated by cognitively demanding tasks that engage the PFC. It is unknown, however, if such an acute down-regulation of amygdala activity might correlate with reduced fear in anxious participants. In an fMRI study of 43 participants (11 men) with fear of snakes, we found reduced amygdala activity when visual stimuli were processed under high cognitive load, irrespective of whether the stimuli were of neutral or phobic content. Furthermore, dynamic causal modeling revealed that this general reduction in amygdala activity was partially mediated by a load-dependent increase in dorsolateral PFC activity. Importantly, high cognitive load also resulted in an acute decrease in perceived phobic fear while viewing the fearful stimuli. In conclusion, our data indicate that a cognitively demanding task results in a top–down regulation of amygdala activity and an acute reduction of fear in phobic participants. These findings may inspire the development of novel psychological intervention approaches aimed at reducing fear in anxiety disorders. ■

INTRODUCTION

The amygdala is fundamentally involved in processing emotional stimuli of positive and negative valence (Janak & Tye, 2015), including fear in animals (Fanselow & Gale, 2003; Davis & Whalen, 2001) and humans (Shin & Liberzon, 2010; LeDoux, 2007; Adolphs, Tranel, Damasio, & Damasio, 1995). Furthermore, amygdala hyperactivity has been associated with many anxiety disorders including phobias. Specifically, phobic participants show higher amygdala activation compared with healthy participants when confronted with phobic stimuli (Ipser, Singh, & Stein, 2013; Straube, Mentzel, & Miltner, 2006; Schienle, Schäfer, Walter, Stark, & Vaitl, 2005; Dilger et al., 2003). Proper regulation of emotional reactions, including a down-regulation of fear, is thought to rely on the successful interplay between prefrontal and limbic regions (Okon-Singer, Hendler, Pessoa, & Shackman, 2015; Dolcos & Denkova, 2014; Pessoa, 2013). Within the prefrontal network, the dorsolateral PFC (dlPFC) is critically involved in higher cognitive processes like working memory and executive control (Kohn et al., 2014; Barbey, Koenigs, & Grafman, 2013; Owen, McMillan, Laird, & Bullmore, 2005; Curtis & D'Esposito, 2003) and has been reported to interact with regions engaged in emotion processing and emotion regulation (Dolcos, Iordan, & Dolcos, 2011; Van Dillen, Heslenfeld, & Koole, 2009; Ochsner & Gross, 2005; Phillips, Drevets, Rauch, & Lane, 2003). fMRI studies have consistently shown that cognitively demanding tasks are associated with increased dlPFC activity and decreased amygdala activity (de Voogd et al., 2018; Straube, Lipka, Sauer, Mothes-Lasch, & Miltner, 2011; Erk, Kleczar, & Walter, 2007; Mitchell et al., 2007). In situations that demand high cognitive functioning, the dlPFC is assumed to inhibit limbic regions, including the amygdala through top–down control mechanisms, to ensure that emotional reactions do not interfere with goal-directed behavior (Okon-Singer et al., 2015; Clarke & Johnstone, 2013; Iordan, Dolcos, & Dolcos, 2013). On a behavioral level, increased cognitive load has been associated with reduced state anxiety and startle response (Balderston et al., 2016; Vytal, Arkin, Overstreet, Lieberman, & Grillon, 2016; Vytal, Cornwell, Arkin, & Grillon, 2012; King & Schaefer, 2011) and with reduced subjectively experienced negative emotion in response to negative stimuli (Van Dillen et al., 2009). Additionally, performing a cognitively demanding task over several weeks resulted in better cognitive control in healthy (Cohen et al., 2016; Schweizer, Grahn, Hampshire, Mobbs, & Dalgleish, 2013; Schweizer, Hampshire, & Dalgleish, 2011) as well as in anxious individuals (Sari, Koster, Pourtois, & Derakshan, 2016).

To our knowledge, it has not yet been investigated whether a cognitively demanding task known to engage the dlPFC could be used to acutely decrease amygdala activity and reduce subjectively felt fear in anxious participants.

University of Basel
*These authors contributed equally to this work.

To address this question, we designed a pictorial *n*-back task and measured amygdala activity during the viewing of snake pictures and neutral pictures in participants with fear of snakes under different cognitive load conditions. The task included a high cognitive load condition (2-back) and a low cognitive load condition (0-back), whereby the snake pictures and neutral pictures served as targets in the different conditions (Figure 1). This design ensured that the visual input during the *n*-back task was identical across load conditions. We hypothesized reduced amygdala activity and reduced subjective fear ratings during the high load condition, as compared with the low load condition. Additionally, we applied dynamic causal modeling (DCM) to investigate a possible load-dependent change in effective connectivity between the dlPFC and the amygdala.

METHODS

Participants

Forty-three participants (11 men; mean age = 23.12 years, *SD* = 3.37 years) were included in the final analysis after removing four participants because of corrupted fMRI data (in three participants, there was a mistake in the scanning procedure, and one participant displayed excessive head motions, which resulted in poor quality of the imaging data). Another participant was excluded because of low fear ratings of the snake pictures during the pictorial *n*-back task (> 2.5 *SD* from sample mean).

Participants were recruited from the Basel and Zurich area in Switzerland through advertisements on the Internet, trams, and buses as well as through distribution of flyers. Participants had to meet the following inclusion criteria: (1) age between 18 and 35 years, (2) body mass index between 18 (women)/19 (men) and 35 kg/m^2, (3) native or fluent German-speaking, (4) capable of viewing pictures of snakes without turning the head away, and (5) a score of 12 or higher in a snake anxiety questionnaire (Schlangenangst Screening [fear of snakes screening]; SCANS questionnaire; Reinecke, Hoyer, Rinck, & Becker, 2009). The SCANS is a short and time-efficient self-report questionnaire consisting of four items pertaining to the four relevant *Diagnostic and Statistical Manual of Mental Disorders IV* (DSM-IV) diagnosis criteria of snake phobia (persistent fear, anxiety response, avoidance, distress). Participants judge each statement on a 7-point Likert scale (0–6). Reinecke et al. (2009) reported that the SCANS discriminated well between participants fulfilling DSM-IV criteria for specific phobia and healthy controls. Although controls showed a mean SCANS score of 1.5 (*SD* = 1.8), participants with fear of snakes showed a mean score of 18.3 (*SD* = 2.3). In our sample, the mean SCANS score was 17.51 (*Mdn* = 18, *SD* = 3.04, range = 12–23), indicating medium to high fear of snakes. With regard to psychometric properties, the SCANS shows a good test–retest reliability (r = .84) as well as high correlations with other snake questionnaires (convergent validity) like the Snake Anxiety Questionnaire (Klorman, Weerts, Hastings, Melamed, & Lang, 1974; r = .76) or the Aspects of Snake Fear Questionnaire (Suedfeld & Hare, 1977; r = .87).

Participants were free of any neurological or psychiatric illness (except the fear of snakes), did not take any medication at the time of the experiment (oral contraception was allowed), and had normal or corrected-to-normal vision. Participants gave their written informed consent to participate in the study, which was approved by the Ethics Committee of Northwest/Central Switzerland (Registration Number BASEC 2016-01330). All participants received 25 CHF/hr as compensation for their participation.

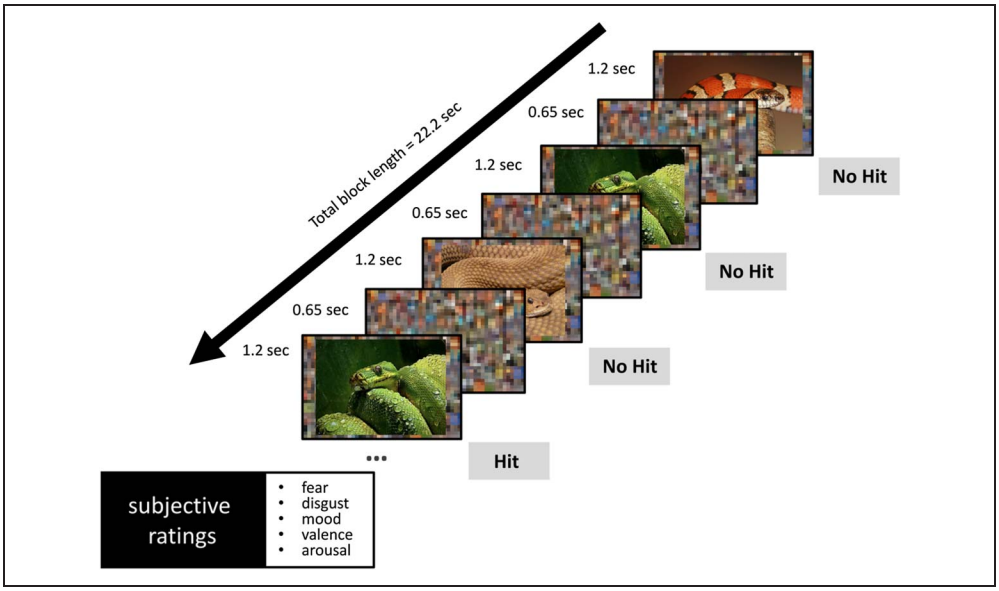

Figure 1. *n*-back task performed during fMRI. The figure illustrates a 2-back task block with snake pictures. Participants had to remember the snake picture presented two positions before and indicate if the currently presented picture was the same (Hit) or a different one (No Hit). During 0-back blocks, a target picture was presented at the beginning of each block, and participants had to respond each time it was presented during the block. For the 2-back and 0-back neutral condition, snake pictures were replaced by pictures of neutral objects. In total, each participant completed 32 *n*-back task blocks (eight blocks of each condition: 0-back/snake, 2-back/snake, 0-back/neutral, and 2-back/neutral).

Stimuli and Task Description

Description of the Pictorial n-back Task

The task designed for this study was a pictorial *n*-back task consisting of two levels of cognitive load (low load: 0-back; high load: 2-back) and two types of pictures (snake pictures, neutral pictures), resulting in four conditions for each participant (within-participant design): (1) 0-back/snake, (2) 2-back/snake, (3) 0-back/neutral, and (4) 2-back/neutral (see Figure 1).

During the 0-back conditions, participants needed to respond as quickly as possible to the occurrence of a target picture (snake or neutral). The 0-back mainly requires general attention processes (Owen et al., 2005) and is thus considered to induce only low task load. In the 2-back condition, participants had to judge whether the currently presented picture was identical to the one presented two positions before. The 2-back condition served as a high load condition because it requires online monitoring, updating, and manipulation of remembered information (Owen et al., 2005).

In total, the task comprised 32 blocks (eight blocks per condition), presented in a quasi-randomized order. In each block, four different pictures of the same picture type were quasi-randomly presented three times, resulting in a total of 12 presented pictures per block. Each block contained three target stimuli and nine nontarget stimuli, resulting in a target rate of 25%. Participants had to react to these targets as quickly as possible. At the beginning of each block, an introduction was displayed for 5 sec to introduce the next task (0-back or 2-back). In case of a 0-back condition, the instruction also comprised a randomly selected picture that served as a target in the following block. After the instruction, a black screen appeared for 1 sec before the block started. Pictures were presented on a scrambled background for 1.2 sec, with only scrambled background between pictures (0.65 sec). Every block lasted for 22.2 sec.

After each block, participants had to rate how they had felt during the last block on five separate visual analog scales via button presses (see Emotion Ratings during *n*-back Task section). The ratings lasted for a total of 40 sec. After a break (random duration, min = 1 sec and max = 8 sec; 20 sec in total over four consecutive blocks), an empty screen was presented for 1 sec until the instructions of the next task block appeared.

Conditions were presented in a quasi-randomized order, that is, each of the four conditions was presented once before being presented again. Furthermore, snake and neutral pictures were assigned to 0-back and 2-back blocks in a counterbalanced fashion. As blocks of snake pictures always depicted the same animal (snake), we took care that neutral pictures also depicted the same type of object within one task block (e.g., chairs) to control blocks for task difficulty. However, the type of neutral object changed for each new task block.

Picture Selection

In total, 64 pictures of snakes and 64 pictures depicting neutral objects were used in this study. All snake pictures and 21 neutral pictures were selected from the Geneva Affective Picture System (Dan-Glauser & Scherer, 2011), and 24 neutral pictures were from the International Affective Picture System (Lang, Bradley, & Cuthbert, 2008). Because these standard picture systems did not provide us with a sufficient number of neutral pictures in accordance with our selection criteria, we selected 19 additional neutral pictures from in-house standardized picture sets. Neutral pictures comprised single inanimate objects like chairs, clocks, cups, or shoes. With regard to visual complexity, these pictures were comparable to each other as well as to the selected snake pictures.

Emotion Ratings during n-back Task

To measure participants' emotional reaction to the pictures presented during the task blocks, five separate visual rating scales (11-point Likert scales) were presented after each block. An instruction slide appeared for 5 sec, announcing the first three ratings. Afterward, participants had to indicate how much fear (none–maximal) and how much disgust (none–maximal) they had felt during the last task block as well as the state of their mood (very good–very bad). In total, the participants were given 18 sec to indicate their ratings (on average 6 sec per rating) by moving the curser stepwise to the according scale position on an fMRI-compatible finger-controlled button box. If participants were faster than 18 sec, a cross appeared in the middle of the screen for the remaining time. Next, a second instruction slide appeared for 5 sec, announcing the last two ratings. Participants rated the pictures of the last block according to overall valence (positive–negative) and arousal (low–high). Participants were given a total of 12 sec to indicate their ratings (6 sec per rating).

Experimental Procedure

Before the day of the experiment, participants received general information about the study and filled out an online questionnaire to assess study eligibility. The software SoSci Survey was used for online assessments (Leiner, 2014).

The experiment took place at the University Hospital of Basel. Upon arrival, participants gave written informed consent. They were then trained on the *n*-back task. Only neutral pictures were used for training. The training was repeated if the number of correct responses was lower than 90% in the 0-back or lower than 70% in the 2-back. Afterward, participants entered the scanner. All participants received earplugs and headphones during MR scans to reduce scanner noise and were instructed not to move during the scans. Small foam pads were used for additional head fixation. We used MR-compatible

LCD goggles (VisualSystem, NordicNeuroLab) to present the *n*-back task inside the scanner and to track eye movements during the task. Eye-tracking data were acquired with the ViewPoint eyetracker software (Arrington Research), and calibration was done at the beginning of the experiment. Vision correction was used if necessary. Participants gave their responses via a button box placed on their lower abdomen using the index, middle, and ring finger of their dominant hand. The *n*-back task lasted 40 min and was followed by 10 min of magnetization-prepared rapid gradient-echo and B0 field map acquisition.

We used Presentation software (Version 14.5; Neurobehavioral Systems, Inc., www.neurobs.com) to present the tasks inside the scanner.

Statistical Analysis of the Behavioral Data

All statistical analyses of behavioral data were performed in R (Version 3.3.2; RRID:SCR_001905) by using linear mixed models in combination with ANOVA. The two within-participant factors Cognitive Load (0-back, 2-back) and Picture Type (snake, neutral), as well as the interaction between Cognitive Load and Picture Type, were entered into the model. In case of a significant interaction, post hoc tests were applied separately for each picture type. Participant-IDs were included as random effect. In case that model assumptions were not met (visual inspection of normal distribution and random intercept, Shapiro–Wilk normality test), we used nonparametric two-way repeated ANOVA by means of ANOVA-type statistic (ATS) as provided in the R package *nparLD* (Noguchi, Gel, Brunner, & Konietschke, 2012). The ATS rank-based method tests the hypothesis of equality of distributions rather than the equality of means (Shah & Madden, 2004).

Assessment of n-back Performance

To assess whether 2-back blocks were more demanding and therefore induced a higher cognitive load than 0-back blocks, we measured participants' task performance, that is, accuracy (hits plus correct rejections divided by the total number of pictures shown) and d' (Stanislaw & Todorov, 1999) measures. Two separate statistical models were calculated, with accuracy and d' serving as dependent variables.

Preprocessing and Analysis of Eye-tracking Data

For each participant, fixation detection was performed with an individual, velocity-based algorithm using the *saccades* package (von der Malsburg, 2015) and a lower fixation duration threshold of 100 msec. The analysis was restricted to ROIs, which were manually defined for each picture as the region covered by the main object in the picture (e.g., a snake or a chair; opposed to the background of the picture). The average dwell time in a ROI was calculated for each task condition to quantify the overt attention drawn to these regions.

Analysis of Emotion Ratings during n-back Task

As an experimental manipulation check, we first investigated for each emotion rating whether snake pictures, on average, induced more negative emotions than neutral pictures, irrespective of cognitive load. Here, we calculated separate dependent two-sided *t* tests for each rating of the *n*-back task.

Our main analyses of interest (interaction of Cognitive Load × Picture Type and effect of load) were performed by using separate statistical models for each of the emotion ratings.

As the rating of fear during the *n*-back task constituted our primary variable of interest, we set the significance threshold to $p < .05$ for this rating. Bonferroni correction was implemented to account for multiple testing for all remaining ratings (disgust, mood, valence, and arousal; Bonferroni correction for four independent tests).

fMRI Data Acquisition

Measurements were performed on a Siemens Magnetom SkyraFit 3 T whole-body MR unit equipped with a 32-channel head coil. Functional series were acquired using a single-shot echo-planar sequence using parallel imaging (Generalized Autocalibrating Partial Parallel Acquisition; GRAPPA). The following acquisition parameters were applied: echo time (TE) = 30 msec, field of view = 24 cm, acquisition matrix = 96 × 96, voxel size = 2.5 × 2.5 × 3 mm^3, GRAPPA acceleration factor $R = 2.0$. Using a mid-sagittal scout image, 42 contiguous axial slices placed along the AC–PC plane covering the entire brain with a repetition time (TR) of 2600 msec ($\alpha = 82°$) were sampled with an ascending interleaved sequence. A high-resolution T1-weighted anatomical image was acquired for each participant using a magnetization-prepared rapid gradient echo (TR = 2000 msec, TE = 2.26 msec, inversion time = 1000 msec, flip angle = 8°, 176 slices, field of view = 256 mm, voxel size = 1.5 × 1.5 × 1.5 mm^3).

To correct the fMRI data for geometric distortions caused by magnetic field inhomogeneities, B0 field-map scans were collected as well (TR = 550 msec, TE = 4.92 msec/7.38 msec, flip angle = 60°, voxel size = 2.5 × 2.5 × 3.0 mm^3).

Processing of Structural MRI Data and Construction of Probabilistic Atlas

Each participant's anatomical image was automatically segmented into cortical and subcortical structures using FreeSurfer v5.3.0 (Fischl et al., 2002). Labeling of the cortical gyri was based on the Desikan–Killiany atlas (Desikan et al., 2006), yielding 35 cortical and 7 subcortical regions per hemisphere.

The segmentations were used to build a population-averaged probabilistic anatomical atlas. Individual segmented anatomical images were subsequently normalized to the study-specific anatomical template space using the participant's previously computed warp field and affine-registered to the Montreal Neurological Institute (MNI) space. Nearest-neighbor interpolation was applied to preserve labeling of the different structures. The normalized segmentations were finally averaged across all 43 participants to create a population-averaged probabilistic atlas. Each voxel of the template could consequently be assigned a probability of belonging to a given anatomical structure.

fMRI Data Analysis

Preprocessing and First-level Analysis

Analyses were performed using SPM12 (Version 6470; Statistical Parametric Mapping, Wellcome Trust Centre for Neuroimaging; www.fil.ion.ucl.ac.uk/spm/) implemented in MATLAB R2014b (The Mathworks, Inc.).

To account for magnetization effects, the first four volumes were discarded from further analyses. The remaining volumes were slice-time-corrected to the first slice, realigned and unwarped with the field maps, and coregistred to the anatomical image by applying a normalized mutual information 3-D rigid body transformation. Successful coregistration was visually verified for every participant. Each volume was masked with the participant's T1 anatomical image to exclude voxels outside the brain. The EPI volumes were normalized to MNI space by applying DARTEL, which leads to an improved registration between participants (Klein et al., 2009; Ashburner, 2007). Normalization incorporated the following steps: (1) structural images of each participant were segmented using the "Segment" procedure in SPM12. (2) The resulting gray and white matter images were used to derive a study-specific group template. The template was computed from all participants included in this study ($n = 43$). (3) An affine transformation was applied to map the group template to MNI space. (4) Participant-to-template and template-to-MNI transformations were combined to map the functional images to MNI space. The functional images were smoothed with an isotropic 5-mm FWHM Gaussian filter.

Normalized functional images were masked using information from their respective T1 anatomical file as follows: At first, the three-tissue classification probability maps of the "Segment" procedure (gray matter, white matter, and CSF) were summed to define a brain mask. The mask was binarized, dilated, and eroded with a $3 \times 3 \times 3$ voxels kernel using fslmaths (FSL) to fill in potential small holes in the mask. The previously computed DARTEL flowfield was used to normalize the brain mask to MNI space, at the spatial resolution of the functional images. The resulting nonbinary mask was thresholded at 50% and applied to the normalized functional images. Consequently, the implicit intensity-based masking threshold usually employed to compute a brain mask from the functional data during the first-level specification (*spm_get_defaults('mask.thresh')*, by default fixed at .8) was not required anymore and therefore set to a lower value of .05.

Analyses were conducted in the framework of the general linear model. Intrinsic autocorrelations were accounted for by AR(1), and low-frequency drifts were removed via a high-pass filter (time constant, 128 sec). Regressors, which modeled the onset and duration of each block, were convolved with a canonical hemodynamic response function. Separate regressors were constructed for each of the four *n*-back conditions: (1) 0-back neutral, (2) 0-back snake, (3) 2-back neutral, and (4) 2-back snake. Events between blocks, that is, task instructions, ratings, and breaks, were modeled as separate regressors. Additionally, six movement regressors from spatial realignment were included as regressors of no interest.

The resulting parameter estimates were used to specify contrasts using fixed effects models (first-level analysis). The following contrasts were specified: (1) "picture contrast": brain activity related to presentation of snake pictures compared with neutral pictures (snake pictures–neutral pictures), independently of whether the picture was shown under 0-back or 2-back; (2) "load contrast": brain activity related to pictures presented under 0-back or 2-back (0-back–2-back), irrespective of whether the picture depicted a snake or a neutral object; and (3) "interaction contrast": brain activity related to the interaction of load and picture type ([0-back snake–2-back snake]–[0-back neutral–2-back neutral]).

Group-level Analysis

The single-participant contrast maps of the first-level analysis were entered in a random effects model to make inferences on group level. We controlled for sex and age by including them as covariates. As the amygdala and the dlPFC served as ROIs in this analysis, we applied a small volume correction (SVC) for these regions. We first created one probabilistic mask for the amygdala and one for the dlPFC by combining the respective masks from both hemispheres. These masks were taken from the population-specific atlas (corresponding Freesurfer labels for dlPFC mask: ctx-lh-rostralmiddlefrontal/ctx-rh-rostralmiddlefrontal). The probabilistic masks were consequently thresholded at 50%, binarized and applied to the group-level contrast maps ($p < .05$, family-wise error [FWE]-corrected for multiple comparisons within the mask [$p_{\text{FWE-SVC}}$]).

DCM: Extracting Time Courses from Volumes of Interest

We used DCM to investigate a possible inhibition of amygdala activity through top–down control of prefrontal regions when cognitive load was high. Volumes of interest

(VOIs) were defined as the amygdala and the dlPFC. Time courses were extracted separately per hemisphere.

The applied approach was similar to the one used by Fastenrath et al. (2014). First, we identified local maxima at the group level for each of the four anatomical masks (amygdala and dlPFC from both hemispheres). Local maxima were based on the load contrast (0-back–2-back). Second, group-level coordinates in MNI space were mapped to native participant space. Based on these participant space coordinates, participant-specific local maxima were identified within a distance of 10 mm. Time courses were extracted by computing the principal eigenvariate of the data across all significant voxels ($p <$ .05 uncorrected, minimum cluster size 3) within a 10-mm sphere around the participant-specific local maxima and within the participant-specific anatomical mask (masks were retrieved from the FreeSurfer segmentations). The application of the aforementioned p value threshold of .05 with a minimal cluster size of 3 allowed us to separate voxels with task-related signal from voxels with noisy signal (see, e.g., Stephan et al., 2010). This procedure implies that time series are extracted only from those voxels reaching this threshold. As data from all VOIs in all participants are a prerequisite to run DCM (Stephan et al., 2010; Friston, Harrison, & Penny, 2003), participants who did not show sufficient activation in line with these criteria were excluded from further DCM analysis. Consequently, 9 of 43 participants had to be excluded per hemisphere. The extracted time courses were adjusted to the F contrast (i.e., effects of interest) of each participant and entered into the DCM models.

DCM: Defining Model Space and Model Comparison

We applied bilinear, deterministic DCM with two states (Version DCM12 r6432 in SPM 12 r6470; Marreiros, Kiebel, & Friston, 2008). We ran DCM for the left and right hemispheres separately. In each hemisphere, models were set up consisting of two nodes, corresponding to the amygdala and the dlPFC, respectively. We allowed full bidirectional connectivity between the two nodes. The two load conditions 0-back and 2-back, as well as instructions and emotion ratings, served as driving input to either one of the regions or to both regions. This resulted in three input possibilities to the network, that is, three different models per hemisphere. Within each model, the connections between both regions could be modulated by either the 0-back or the 2-back condition, irrespective of picture type. We focused on the difference in task load because we did not find any significant interaction effect between task load and picture type in the fMRI group-level analysis, which would have been a prerequisite to extract peak coordinates for the DCM analysis.

DCM is based on Bayesian statistics. The model evidence denotes the probability of the data given the model while adjusting for model complexity and dependencies among parameters (Penny et al., 2010; Stephan, Penny, Daunizeau, Moran, & Friston, 2009). Models were compared by conducting random-effects Bayesian model selection (BMS; Penny et al., 2010; Stephan et al., 2009) and differed only in the location of the driving input. This allowed us to test whether one of the models was more likely than any of the other two, which is expressed as exceedance probability.

DCM: Bayesian Model Averaging and Parameter Analysis

Bayesian model averaging (BMA) was applied to obtain a summary measure of likely connectivity values (Penny et al., 2010). The connectivity parameters of each model were weighted by the posterior model probability and subsequently averaged within each participant. Overall, the BMA weighting procedure resulted in participant-specific connectivity estimates that were independent of a particular model while ensuring that models with a high probability contributed more than models with a lower probability.

The BMA modulatory parameter estimates of each participant were further analyzed using R (www.r-project.org). We checked for possible sex and age effects by calculating linear mixed models. As we did not find any significant effects of sex or age ($p > .05$), these variables were not considered in the following analyses.

To test for differences in connectivity strength, we applied the same statistical approach as for the analysis of behavioral data (see Statistical Analysis of the Behavioral Data section). Bonferroni correction was implemented to account for multiple testing (left and right hemisphere; $p < .025$).

RESULTS

Behavioral Results

n-back Performance

Performance in the 0-back condition was significantly better than in the 2-back condition (accuracy: ATS(1) = 261.47, $p < 8.2 \times 10^{-59}$; d': $t(126) = 17.42$, $p < 2.4 \times 10^{-35}$; see also Table 1), indicating effective manipulation of load. There was no significant interaction between Cognitive Load and Picture Type or main effect of Picture Type on n-back performance (accuracy: $p > .07$; d': $p > .19$).

Eye-tracking

We used eye-tracking to investigate if the average dwell time in informative picture regions, as an index for overt attention, varied depending on cognitive load, picture type, or their interaction. Such a difference in overt attention allocation might have affected fear ratings by altering the visual input of fear-inducing information.

For the average dwell time in ROI of pictures, there was neither an effect of Cognitive Load ($p = .35$) nor of Picture Type ($p = .14$) nor an interaction effect ($p = .42$). This

Table 1. *n*-back Performance (Accuracy, d')

	Neutral Pictures		*Snake Pictures*	
	0-back	*2-back*	*0-back*	*2-back*
Accuracy	0.97 (0.03)	0.86 (0.07)	0.97 (0.04)	0.88 (0.07)
d'	3.57 (0.4)	2.39 (0.58)	3.62 (0.48)	2.51 (0.73)

Depicted are mean and standard deviation (in parentheses).

finding indicates that participants spent an equal amount of time looking at relevant regions of the picture, irrespective of valence and load.

Emotion Ratings

As an experimental manipulation check, we first investigated whether snake pictures induced more negative emotions than neutral pictures, irrespective of cognitive load. Participants reported significantly more fear, $t(42) = 17.16$, $p < 1.4 \times 10^{-20}$; disgust, $t(42) = 20.52$, $p < 1.7 \times 10^{-23}$; negative mood, $t(42) = 10.42$, $p < 3.3 \times 10^{-13}$; negative valence, $t(42) = 11.95$, $p < 4.3 \times 10^{-15}$; and arousal, $t(42) = 12.41$, $p < 1.3 \times 10^{-15}$. after blocks depicting snake pictures compared with neutral pictures, indicating that snake pictures evoked more negative emotions than neutral pictures.

Subsequently, we investigated whether there were any interaction effects between Cognitive Load and Picture Type on emotion ratings and whether emotion ratings differed between levels of cognitive load. We found a significant interaction between Cognitive Load and Picture Type for ratings of fear, ATS(1) = 10.5, $p = .001$, and arousal, ATS(1) = 8.92, $p_{\text{Bonferroni corrected}} = .011$, and a trend for disgust, ATS(1) = 6.0, $p_{\text{Bonferroni corrected}} = .057$, and valence, ATS(1) = 5.54, $p_{\text{Bonferroni corrected}} = .074$, but not for mood, ATS(1) = 4.42, $p_{\text{Bonferroni corrected}} = .14$. Consequently, we analyzed ratings of fear and arousal separately for snake pictures and neutral pictures. We also ran post hoc tests for the remaining emotion ratings. As fear rating served as the primary variable of interest, the respective p value threshold was set to $<.05$ in all analyses, whereas p values for all other ratings (disgust, mood, arousal, and valence) were Bonferroni-corrected to account for multiple testing (see Methods section).

Post hoc tests revealed that snake pictures presented during 2-back blocks evoked less fear, ATS(1) = 8.1, $p = .004$, and less disgust, ATS(1) = 9.13, $p_{\text{Bonferroni corrected}} = .01$, than snake pictures presented during 0-back blocks. No significant effects of Load on mood, valence, or arousal were found (all $p_{\text{Bonferroni corrected}} > .45$; see Table 2).

In contrast, neutral pictures presented during 2-back blocks resulted in higher fear ratings, ATS(1) = 4.84, $p = .028$, than neutral pictures presented during 0-back blocks. This finding could reflect an increased fear of failure during the cognitively demanding task blocks compared with low demanding ones. For all other emotion ratings on neutral pictures, no significant effects of Load were found (all $p_{\text{Bonferroni corrected}} > .17$).

fMRI Results for ROIs

Main Effect of Picture Type

Voxel-wise analysis revealed that the amygdala was bilaterally activated during blocks of snake pictures compared

Table 2. Effect of Cognitive Load on Emotional Ratings of Snake and Neutral Pictures during the *n*-back Task

Emotion Ratings	*0-back*	*2-back*	*2-back–0-back*	*p*
Snake pictures				
Fear	62.14 (17.13)	60.47 (16.52)	−1.68 (3.95)	.004*
Disgust	69.09 (17.59)	66.95 (17.05)	−2.14 (4.39)	.003*
Mood	62.78 (12.09)	62.18 (12.43)	−0.59 (4.52)	.53
Valence	65.93 (11.74)	65.03 (11.00)	−0.90 (3.71)	.36
Arousal	64.68 (15.75)	63.46 (15.46)	−1.22 (5.03)	.11
Neutral pictures				
Fear	8.87 (8.92)	11.42 (10.46)	2.56 (6.67)	.03*
Disgust	7.94 (7.7)	9.35 (8.78)	1.41 (5.62)	.13
Mood	29.87 (14.8)	31.84 (15.55)	1.97 (7.72)	.1
Valence	30.87 (12.69)	32.33 (14.49)	1.45 (6.64)	.06
Arousal	20.98 (14.66)	23.33 (14.5)	2.36 (6.84)	.04

Depicted are mean and standard deviation (in parentheses) of each condition, as well as the difference score and nominal p values for the effect of cognitive load derived by nonparametric ATS.

*For fear ratings, $p < .05$; for all other ratings $p < .125$ (Bonferroni correction for four comparisons).

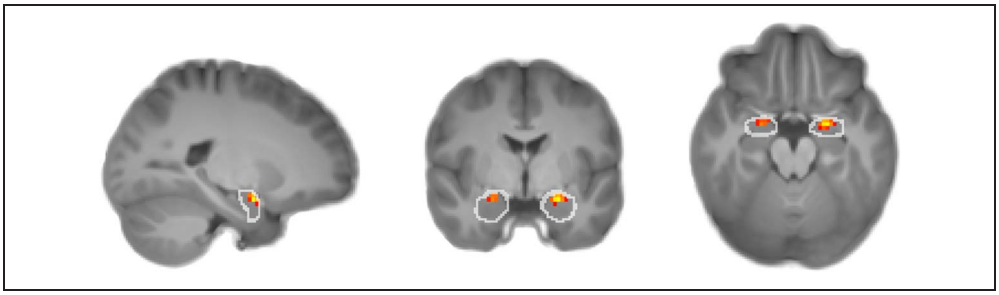

Figure 2. Amygdala activity for the picture contrast (snake pictures–neutral pictures) on group level. Increased amygdala activity during snake pictures as compared with neutral pictures. Depicted are only significant voxels (yellow to red) within the probabilistic amygdala mask (white circles) used for SVC ($p_{FWE\text{-}SVC} < .05$).

with blocks of neutral pictures (peak voxel: left: MNI −22, −2, −18, $t = 6.23$, $k = 23$; right: MNI 22, −2, −18, $t = 4.95$, $k = 10$; $p_{FWE\text{-}SVC} < .05$, corresponding to $t_{SVC} = 3.56$; see Figure 2). The reported activation in the left amygdala also survived whole-brain correction ($t = 5.75$, $p_{FWE} < .05$; see Supplementary Table 1 on whole-brain corrected results[1]). Activation in the same direction was also found in a small cluster in the right dlPFC (peak voxel: MNI −25, 50, 33, $t = 4.72$, $k = 3$), but not in the left dlPFC. We did not observe any effects of sex or age with regard to this activation.

Main Effect of Cognitive Load

Amygdala activity was reduced during 2-back blocks compared with 0-back blocks in both the left hemisphere (peak voxel: MNI −22.5, −10, −15, $t = 8.06$, $k = 73$) and right hemisphere (peak voxel: MNI 22.5, −7.5, −15, $t = 6.71$, $k = 66$; $p_{FWE\text{-}SVC} < .05$, corresponding to $t_{SVC} = 3.5$; see Figure 3A). Furthermore, 2-back blocks resulted in higher bilateral dlPFC activity compared with 0-back blocks (peak voxel: left: MNI −47.5, 25, 33, $t = -10.64$, $k = 640$; right: MNI 45, 30, 39, $t = -11.05$, $k = 357$; $p_{FWE\text{-}SVC} < .05$, corresponding to $t_{SVC} = 4.42$; see Figure 3B). All reported peak activations also survived whole-brain correction ($t = 5.75$, $p_{FWE} < .05$; see Supplementary Tables 2 and 3 on whole-brain corrected results). No significant sex or age effects were found.

Interaction between Cognitive Load and Picture Type

There was no significant interaction effect between cognitive load and picture type on amygdala activity when applying SVC ($p_{FWE\text{-}SVC} > .05$), indicating that there was a similar decrease in amygdala activity during 2-back compared with 0-back for snake pictures and for neutral pictures. No interaction effects were observed for the dlPFC either ($p_{FWE\text{-}SVC} > .05$). Furthermore, we did not observe any whole-brain corrected interaction effects (Cognitive Load × Picture Type).

DCM Results

Extraction of Time Courses in VOIs

Activity in the respective peak voxel within the amygdala and the dlPFC were obtained from the load contrast (0-back–2-back) of the group-level analysis (for peak coordinates, see Table 3). We focused only on the contrast of load as we did not find any interaction

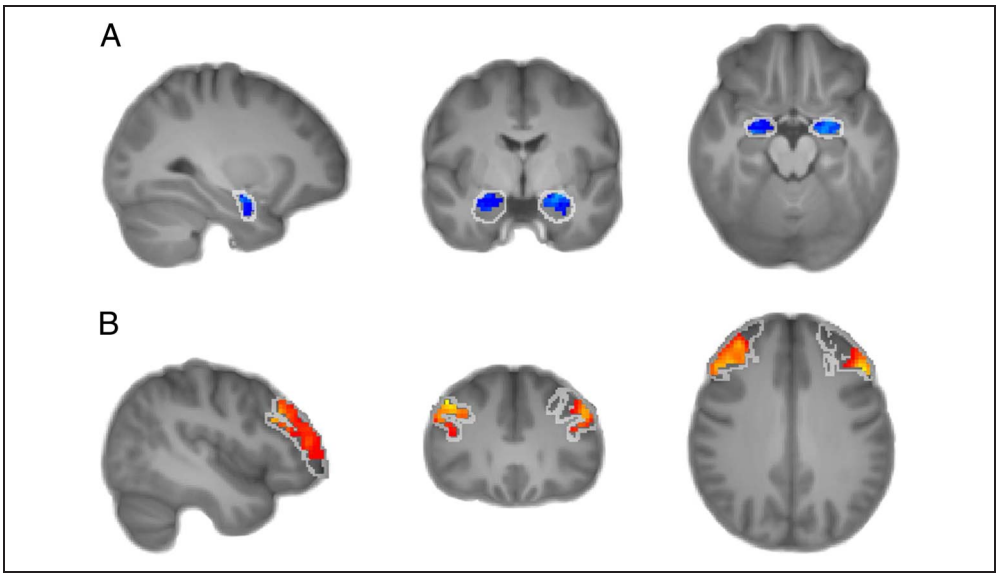

Figure 3. Amygdala and dlPFC activity for the load contrast (0-back–2-back) on group level. Decreased amygdala activity during 2-back blocks as compared with 0-back blocks (A, blue color). Increased dlPFC activity during 2-back blocks as compared with the 0-back blocks (B, yellow to red color). Depicted are significant voxels within the respective probabilistic masks used for SVC ($p_{FWE\text{-}SVC} < .05$).

Table 3. Peak Activation in VOIs Extracted for DCM from the Load Contrast (0-back–2-back) of the Group-level Analysis

Cluster No.	*Max. t Value within Cluster*	*Regional Correspondence of Maximum*	*MNI Coordinates at Maximum*			*No. of Voxels*
			x	*y*	*z*	
1	−8.06	Left amygdala (53%)	−22.5	−10	−15	66
2	−6.71	Right amygdala (86%)	22.5	−7.5	−15	44
3	−10.64	ctx-lh-rostralmiddlefrontal (57%)	−47.5	25	33	640
4	−11.05	ctx-rh-rostralmiddlefrontal (54%)	45	30	39	357

Regions and probabilities are in accordance with population-specific atlas. ctx = cortex; lh = left hemisphere; rh = right hemisphere.

between cognitive load and picture type in the fMRI group-level analysis.

Robust task-related activation in all regions in all participants is a prerequisite to run DCM (see Methods section). Five participants did not show task-related activation, neither in the left nor in the right amygdala. Another four participants did not show task-related activation in the left amygdala and another four participants in the right amygdala. Per hemisphere, time courses were consequently available for 34 of 43 participants.

Model Comparison Using BMS

We constructed three different models based on the site of input to the network. BMS was used to identify the most plausible model given the data. Comparison between the three models indicated that the model where the input entered both regions (amygdala and dlPFC) was most likely (left hemisphere: model exceedance probability = .995; right hemisphere: model exceedance probability = .605) even though there was a considerably high exceedance probability for input only to the dlPFC in the right hemisphere as well (exceedance probability = .395).

Modulatory Influence of Load on Connectivity Parameters

As there was no clearly superior input model for the right hemisphere, we used BMA to calculate connectivity parameters. Modulators of effective connectivity describe whether the strength of the connection (i.e., the influence that one region exerts upon another) increases or decreases under the influence of experimental manipulations (Friston et al., 2003). Modulator estimates were calculated for the 0-back and for the 2-back condition. In addition to modulators of connection strength, DCM also estimates intrinsic connectivity parameters. They represent the connectivity in the absence of experimental perturbations. The effective connection strength associated with the experimental condition can be obtained by adding the value of the intrinsic connection and the value of the modulator. A negative sum indicates that the activity in the source region decreases (inhibits) activity in the target region (Sokolov et al., 2018).

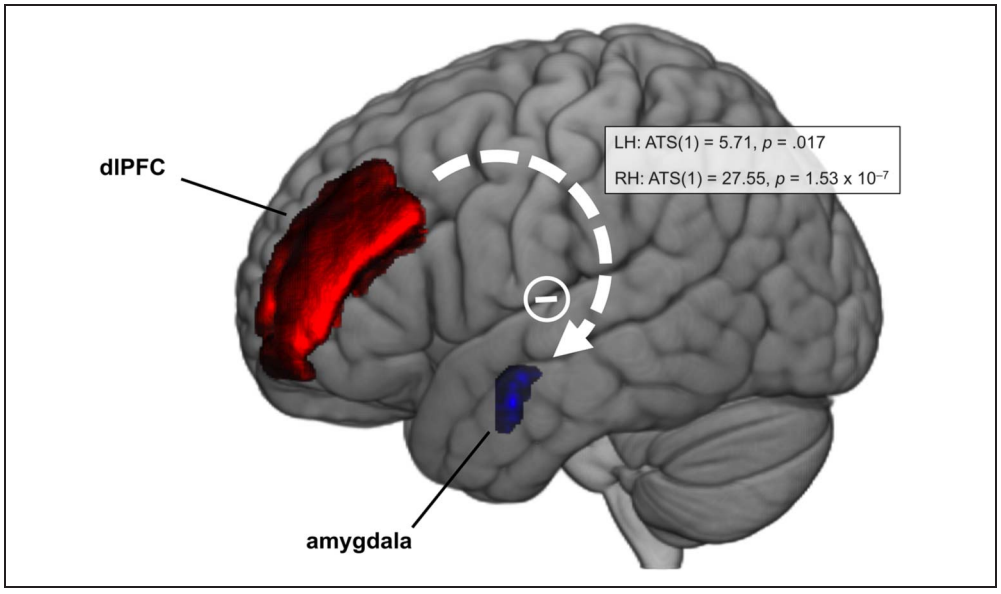

Figure 4. Change in connectivity between the dlPFC (red) and the amygdala (blue) during 2-back blocks compared with 0-back blocks. The white arrow indicates the influence from the dlPFC to the amygdala. The ATS values in the box indicate a stronger decrease in connectivity strength during the 2-back than during the 0-back in the left hemisphere (LH) and the right hemisphere (RH). For parameter values per condition, see Tables 4 and 5.

Table 4. BMA Parameter Values across All 34 Participants in the Left Hemisphere

	Parameter Values (Left Hemisphere)	
Direction of connection	dlPFC to amygdala	Amygdala to dlPFC
Strength of intrinsic connectivity	−0.019 (0.019)	0.020 (0.012)

	0-back	*2-back*	*0-back*	*2-back*
Change in connection strength (modulators) per condition	−0.002 (0.021)	−0.200 (0.066)	−0.015 (0.012)	0.003 (0.012)
Total connectivity	−0.021 (0.035)	−0.219 (0.067)	0.005 (0.020)	0.023 (0.019)

Depicted are mean and *SEM* (in parentheses).

The modulation of connectivity parameters was analyzed on group level. Visual inspection of the data distribution and subsequent statistical testing indicated a deviation from normality in both hemispheres (Shapiro–Wilk test: $p < .05$). For this reason, we report p values of the nonparametric statistical model to ensure robustness of the results.

Modulators of connection strength from the dlPFC to the amygdala differed significantly between the two load conditions in both hemispheres (left: ATS(1) = 5.71, $p = .017$; right: ATS(1) = 27.55, $p = 1.53 \times 10^{-7}$; see Figure 4 and Tables 4 and 5), showing an inhibitory influence of the dlPFC on the amygdala during the 2-back condition. For the direction from the amygdala to the dlPFC, no significant differences in connectivity strength were found between 2-back and 0-back (both hemispheres: $p > .26$).

We performed an additional DCM analysis (based on the same VOIs) that also accounted for possible effects of picture type on functional connectivity between dlPFC and amygdala. This analysis neither revealed a significant interaction effect (both hemispheres: $p > .21$) nor a main effect of picture type (both hemispheres: $p > .11$). The main effect of load remained significant (left: ATS(1) = 28.27, $p = 1.08 \times 10^{-7}$; right: ATS(1) = 51.24, $p = 8.16 \times 10^{-13}$). For the direction from the amygdala to the dlPFC, there was neither a significant interaction effect (both hemispheres: $p > .38$) nor a main effect of cognitive load (both hemispheres: $p > .22$). There was, however, a significant main effect of picture type in the left hemisphere, ATS(1) = 6.92, $p = .009$ ($M_{snake} = 0.015$, $SD = 0.06$; $M_{neutral} = -0.013$, $SD = 0.12$), but not in the right hemisphere ($p = .75$).

DISCUSSION

The confrontation with a feared object or situation typically results in an acute activation of limbic brain regions, including the amygdala, and in perceived fear. In the present fMRI study, we investigated if high cognitive load, induced via a demanding task, would lead to reduced activity of the amygdala as well as to attenuated phobic fear in participants with fear of snakes.

The findings revealed a decrease in amygdala activity during blocks of high cognitive load compared with blocks of low cognitive load. Importantly, we also observed acute effects of cognitive load on subjective fear ratings of snake pictures. When task load was high, participants reported less phobic fear in the presence of fearful pictures. To our knowledge, these results are the first to indicate that engaging in a highly demanding cognitive task can acutely decrease perceived fear toward phobic stimuli.

Applying DCM, we additionally investigated load-depended changes in functional connectivity between the dlPFC and the amygdala. We focused on the effect of task load in the DCM analysis as we did not detect any significant interaction effects between task load and picture type in the initial group-level analysis. This suggests

Table 5. BMA Parameter Values across All 34 Participants in the Right Hemisphere

	Parameter Values (Right Hemisphere)	
Direction of connection	dlPFC to amygdala	Amygdala to dlPFC
Strength of intrinsic connectivity	0.014 (0.047)	0.075 (0.050)

	0-back	*2-back*	*0-back*	*2-back*
Change in connection strength (modulators) per condition	0.056 (0.031)	−0.316 (0.078)	0.006 (0.011)	0.005 (0.024)
Total connectivity	0.071 (0.064)	−0.301 (0.110)	0.081 (0.053)	0.080 (0.040)

Depicted are mean and *SEM* (in parentheses).

a load-dependent decrease in amygdala activation irrespective of whether the presented pictures depicted fearful or neutral objects. This parallels findings from previous experiments in which solving a difficult task has been associated with a decrease in amygdala activity, independently of whether neutral or emotional stimuli were used (Cohen et al., 2016; Straube et al., 2011; Silvert et al., 2007). Our DCM analysis revealed a bilateral decrease in connectivity strength from the dlPFC to the amygdala during high cognitive load compared with low task load, indicating that the dlPFC exerted a stronger inhibitory influence on the amygdala when task demand was high.

What might be the mechanism(s) of the observed reduction of phobic fear under high cognitive load? One potential explanation for reduced amygdala activity and fear is that the high-load condition caused a visual distraction from the emotional pictures. However, as the pictures were used as targets in the *n*-back task, participants were "forced" to process the pictorial information in both load conditions. Our eye-tracking results indicate that, in the current design, participants spent a similar amount of time in the emotional ROIs of the snake pictures in both load conditions. Thus, reduced amygdala activity and fear as a consequence of visual distraction from emotional hotspots appears unlikely. This is in line with a study indicating that cognitive load does not alter dwell time on anxiety-related stimuli (Berggren, Koster, & Derakshan, 2012; see also MacNamara & Proudfit, 2014; Berggren, Richards, Taylor, & Derakshan, 2013). Instead, we argue that the observed fear reduction may have been a result of a load-induced top–down control mechanism, that is, an increase in dlPFC activity when participants engage in a cognitively demanding task induces a decrease in amygdala activity (Okon-Singer et al., 2015). In line with this idea, the current study found that reduced amygdala activation during high load could be explained by a change in effective connectivity between lateral prefrontal regions and the amygdala. The purpose for such a top–down regulation of amygdala activity might be the reallocation of resources from emotional processes to the cognitive task. It has been shown that the presentation of a distractor during a highly demanding task results in a competition for limited cognitive resources (Lavie, 2010; Lavie, Hirst, De Fockert, & Viding, 2004; Desimone & Duncan, 1995). Attention is directed toward accomplishing the cognitively demanding task, leaving little capacity to process the emotional stimulus, which in turn results in attenuated neuronal and behavioral reactions toward emotional stimuli (Balderston et al., 2016; Vytal et al., 2012; Mitchell et al., 2007; Bishop, Jenkins, & Lawrence, 2006). Even though it has been shown that the dlPFC does not have strong direct anatomical connections to the entire amygdala (Ray & Zald, 2012), studies suggest that the dlPFC might functionally interact with the amygdala either through direct projections to the basal nucleus of the amygdala (Birn et al., 2014) or over indirect pathways via the subgenual cingulate gyrus, dorsal ACC, OFC, or ventrolateral PFC (Clarke & Johnstone, 2013; Sladky et al., 2013; Ray & Zald, 2012). The investigation of potential mediating brain regions by load-dependent functional connectivity is interesting and should be considered in future studies examining top–down regulation effects on amygdala activity. Also, the use of TMS could reveal new insights about the involvement of specific cortical regions in processing stimuli under high cognitive load (see, e.g., Schicktanz et al., 2015). Taken together, the mechanism of reduced amygdala activity and reduced fear under high cognitive load may involve a top–down regulation and a reallocation of cognitive resources.

In summary, the findings of this study suggest that high cognitive load, induced by an *n*-back task comprising fearful stimuli, not only decreases amygdala activity but also reduces perceived phobic fear toward fearful stimuli. Future studies may investigate the acute effects of even higher load conditions on amygdala activity and fear. Furthermore, it would be interesting to look into the therapeutic potential of cognitive tasks in anxiety. It has been reported that distraction from anxiogenic stimuli might be a promising approach to treat anxiety-related disorders (see, e.g., Price, Paul, Schneider, & Siegle, 2013; Vytal et al., 2012; Oliver & Page, 2003). Our study now points to an additional beneficial effect of tasks involving high cognitive load, leading to a top–down regulation of amygdala activity and fear. Repeated exposure to phobic stimuli paired with reduced amygdala activity and reduced fear might facilitate fear extinction. In support of this idea, it has recently been shown that extinction learning can be improved in states of reduced amygdala activity (de Voogd et al., 2018). Thus, our findings might contribute to the development of novel psychological treatment approaches aimed at reducing fear in anxiety disorders.

Acknowledgments

The study was funded by the Transfaculty Research Platform Molecular and Cognitive Neurosciences, University of Basel, Switzerland.

Reprint requests should be sent to Dominique de Quervain, Division of Cognitive Neuroscience, University of Basel, Birmannsgasse 8, CH-4055 Basel, or via e-mail: dominique.dequervain@unibas.ch.

Note

1. All three Supplementary Tables, as well as most relevant scripts for first and second level analysis, and DCM analysis can be accessed via this link: https://osf.io/rtz3d/?view_only=218b422676334ef6b4cb13024afc5b53. Furthermore, second level contrasts for analysis of cognitive load, picture type and their interaction can be found on Neurovault: https://neurovault.org/collections/FFXEDLNE/.

REFERENCES

Adolphs, R., Tranel, D., Damasio, H., & Damasio, A. R. (1995). Fear and the human amygdala. *Journal of Neuroscience*, *15*, 5879–5891.

Ashburner, J. (2007). A fast diffeomorphic image registration algorithm. *Neuroimage*, *38*, 95–113.
Balderston, N. L., Quispe-Escudero, D., Hale, E., Davis, A., O'Connell, K., Ernst, M., et al. (2016). Working memory maintenance is sufficient to reduce state anxiety. *Psychophysiology*, *53*, 1660–1668.
Barbey, A. K., Koenigs, M., & Grafman, J. (2013). Dorsolateral prefrontal contributions to human working memory. *Cortex*, *49*, 1195–1205.
Berggren, N., Koster, E. H., & Derakshan, N. (2012). The effect of cognitive load in emotional attention and trait anxiety: An eye movement study. *Journal of Cognitive Psychology*, *24*, 79–91.
Berggren, N., Richards, A., Taylor, J., & Derakshan, N. (2013). Affective attention under cognitive load: Reduced emotional biases but emergent anxiety-related costs to inhibitory control. *Frontiers in Human Neuroscience*, *7*, 188.
Birn, R. M., Shackman, A. J., Oler, J. A., Williams, L. E., McFarlin, D. R., Rogers, G. M., et al. (2014). Evolutionarily conserved prefrontal-amygdalar dysfunction in early-life anxiety. *Molecular Psychiatry*, *19*, 915–922.
Bishop, S. J., Jenkins, R., & Lawrence, A. D. (2006). Neural processing of fearful faces: Effects of anxiety are gated by perceptual capacity limitations. *Cerebral Cortex*, *17*, 1595–1603.
Clarke, R. J., & Johnstone, T. (2013). Prefrontal inhibition of threat processing reduces working memory interference. *Frontiers in Human Neuroscience*, *7*, 228.
Cohen, N., Margulies, D. S., Ashkenazi, S., Schäfer, A., Taubert, M., Henik, A., et al. (2016). Using executive control training to suppress amygdala reactivity to aversive information. *Neuroimage*, *125*, 1022–1031.
Curtis, C. E., & D'Esposito, M. (2003). Persistent activity in the prefrontal cortex during working memory. *Trends in Cognitive Sciences*, *7*, 415–423.
Dan-Glauser, E. S., & Scherer, K. R. (2011). The Geneva Affective Picture Database (GAPED): A new 730-picture database focusing on valence and normative significance. *Behavior Research Methods*, *43*, 468–477.
Davis, M., & Whalen, P. J. (2001). The amygdala: Vigilance and emotion. *Molecular Psychiatry*, *6*, 13–34.
de Voogd, L. D., Kanen, J. W., Neville, D. A., Roelofs, K., Fernández, G., & Hermans, E. J. (2018). Eye-movement intervention enhances extinction via amygdala deactivation. *Journal of Neuroscience*, *38*, 8694–8706.
Desikan, R. S., Ségonne, F., Fischl, B., Quinn, B. T., Dickerson, B. C., Blacker, D., et al. (2006). An automated labeling system for subdividing the human cerebral cortex on MRI scans into gyral based regions of interest. *Neuroimage*, *31*, 968–980.
Desimone, R., & Duncan, J. (1995). Neural mechanisms of selective visual attention. *Annual Review of Neuroscience*, *18*, 193–222.
Dilger, S., Straube, T., Mentzel, H.-J., Fitzek, C., Reichenbach, J. R., Hecht, H., et al. (2003). Brain activation to phobia-related pictures in spider phobic humans: An event-related functional magnetic resonance imaging study. *Neuroscience Letters*, *348*, 29–32.
Dolcos, F., & Denkova, E. (2014). Current emotion research in cognitive neuroscience: Linking enhancing and impairing effects of emotion on cognition. *Emotion Review*, *6*, 362–375.
Dolcos, F., Iordan, A. D., & Dolcos, S. (2011). Neural correlates of emotion–cognition interactions: A review of evidence from brain imaging investigations. *Journal of Cognitive Psychology*, *23*, 669–694.
Erk, S., Kleczar, A., & Walter, H. (2007). Valence-specific regulation effects in a working memory task with emotional context. *Neuroimage*, *37*, 623–632.
Fanselow, M. S., & Gale, G. D. (2003). The amygdala, fear, and memory. *Annals of the New York Academy of Sciences*, *985*, 125–134.
Fastenrath, M., Coynel, D., Spalek, K., Milnik, A., Gschwind, L., Roozendaal, B., et al. (2014). Dynamic modulation of amygdala–hippocampal connectivity by emotional arousal. *Journal of Neuroscience*, *34*, 13935–13947.
Fischl, B., Salat, D. H., Busa, E., Albert, M., Dieterich, M., Haselgrove, C., et al. (2002). Whole brain segmentation: Automated labeling of neuroanatomical structures in the human brain. *Neuron*, *33*, 341–355.
Friston, K. J., Harrison, L., & Penny, W. (2003). Dynamic causal modelling. *Neuroimage*, *19*, 1273–1302.
Iordan, A. D., Dolcos, S., & Dolcos, F. (2013). Neural signatures of the response to emotional distraction: A review of evidence from brain imaging investigations. *Frontiers in Human Neuroscience*, *7*, 200.
Ipser, J. C., Singh, L., & Stein, D. J. (2013). Meta-analysis of functional brain imaging in specific phobia. *Psychiatry and Clinical Neurosciences*, *67*, 311–322.
Janak, P. H., & Tye, K. M. (2015). From circuits to behaviour in the amygdala. *Nature*, *517*, 284–292.
King, R., & Schaefer, A. (2011). The emotional startle effect is disrupted by a concurrent working memory task. *Psychophysiology*, *48*, 269–272.
Klein, A., Andersson, J., Ardekani, B. A., Ashburner, J., Avants, B., Chiang, M. C., et al. (2009). Evaluation of 14 nonlinear deformation algorithms applied to human brain MRI registration. *Neuroimage*, *46*, 786–802.
Klorman, R., Weerts, T. C., Hastings, J. E., Melamed, B. G., & Lang, P. J. (1974). Psychometric description of some specific-fear questionnaires. *Behavior Therapy*, *5*, 401–409.
Kohn, N., Eickhoff, S. B., Scheller, M., Laird, A. R., Fox, P. T., & Habel, U. (2014). Neural network of cognitive emotion regulation—An ALE meta-analysis and MACM analysis. *Neuroimage*, *87*, 345–355.
Lang, P. J., Bradley, M. M., & Cuthbert, B. N. (2008). *International Affective Picture System (IAPS): Affective ratings of pictures and instruction manual*. Gainesville, FL: University of Florida.
Lavie, N. (2010). Attention, distraction, and cognitive control under load. *Current Directions in Psychological Science*, *19*, 143–148.
Lavie, N., Hirst, A., De Fockert, J. W., & Viding, E. (2004). Load theory of selective attention and cognitive control. *Journal of Experimental Psychology: General*, *133*, 339–354.
LeDoux, J. (2007). The amygdala. *Current Biology*, *17*, R868–R874.
Leiner, D. J. (2014). SoSci Survey (Version 2.5.00-i) [Computer software]. https://www.soscisurvey.de/.
MacNamara, A., & Proudfit, G. H. (2014). Cognitive load and emotional processing in generalized anxiety disorder: Electrocortical evidence for increased distractibility. *Journal of Abnormal Psychology*, *123*, 557–565.
Marreiros, A. C., Kiebel, S. J., & Friston, K. J. (2008). Dynamic causal modelling for fMRI: A two-state model. *Neuroimage*, *39*, 269–278.
Mitchell, D. G., Nakic, M., Fridberg, D., Kamel, N., Pine, D., & Blair, R. (2007). The impact of processing load on emotion. *Neuroimage*, *34*, 1299–1309.
Noguchi, K., Gel, Y. R., Brunner, E., & Konietschke, F. (2012). nparLD: An R software package for the nonparametric analysis of longitudinal data in factorial experiments. *Journal of Statistical Software*, *50*, 1–23.
Ochsner, K. N., & Gross, J. J. (2005). The cognitive control of emotion. *Trends in Cognitive Sciences*, *9*, 242–249.
Okon-Singer, H., Hendler, T., Pessoa, L., & Shackman, A. J. (2015). The neurobiology of emotion–cognition interactions: Fundamental questions and strategies for future research. *Frontiers in Human Neuroscience*, *9*, 58.
Oliver, N. S., & Page, A. C. (2003). Fear reduction during in vivo exposure to blood-injection stimuli: Distraction vs. attentional focus. *British Journal of Clinical Psychology*, *42*, 13–25.

Owen, A. M., McMillan, K. M., Laird, A. R., & Bullmore, E. (2005). *n*-back working memory paradigm: A meta-analysis of normative functional neuroimaging studies. *Human Brain Mapping*, *25*, 46–59.

Penny, W. D., Stephan, K. E., Daunizeau, J., Rosa, M. J., Friston, K. J., Schofield, T. M., et al. (2010). Comparing families of dynamic causal models. *PLoS Computational Biology*, *6*, e1000709.

Pessoa, L. (2013). *The cognitive-emotional brain: From interactions to integration*. Cambridge, MA: MIT Press.

Phillips, M. L., Drevets, W. C., Rauch, S. L., & Lane, R. (2003). Neurobiology of emotion perception I: The neural basis of normal emotion perception. *Biological Psychiatry*, *54*, 504–514.

Price, R. B., Paul, B., Schneider, W., & Siegle, G. J. (2013). Neural correlates of three neurocognitive intervention strategies: A preliminary step towards personalized treatment for psychological disorders. *Cognitive Therapy and Research*, *37*, 657–672.

Ray, R. D., & Zald, D. H. (2012). Anatomical insights into the interaction of emotion and cognition in the prefrontal cortex. *Neuroscience & Biobehavioral Reviews*, *36*, 479–501.

Reinecke, A., Hoyer, J., Rinck, M., & Becker, E. S. (2009). Zwei kurzscreenings zur messung von angst vor schlangen: Reliabilität und validität im vergleich zum SNAQ [Two short-screenings measuring fear of snakes: Reliability and validity by contrast with the SNAQ]. *Klinische Diagnostik und Evaluation*, *2*, 221–239.

Sari, B. A., Koster, E. H., Pourtois, G., & Derakshan, N. (2016). Training working memory to improve attentional control in anxiety: A proof-of-principle study using behavioral and electrophysiological measures. *Biological Psychology*, *121*, 203–212.

Schicktanz, N., Fastenrath, M., Milnik, A., Spalek, K., Auschra, B., Nyffeler, T., et al. (2015). Continuous theta burst stimulation over the left dorsolateral prefrontal cortex decreases medium load working memory performance in healthy humans. *PLoS One*, *10*, e0120640.

Schienle, A., Schäfer, A., Walter, B., Stark, R., & Vaitl, D. (2005). Brain activation of spider phobics towards disorder-relevant, generally disgust- and fear-inducing pictures. *Neuroscience Letters*, *388*, 1–6.

Schweizer, S., Grahn, J., Hampshire, A., Mobbs, D., & Dalgleish, T. (2013). Training the emotional brain: Improving affective control through emotional working memory training. *Journal of Neuroscience*, *33*, 5301–5311.

Schweizer, S., Hampshire, A., & Dalgleish, T. (2011). Extending brain-training to the affective domain: Increasing cognitive and affective executive control through emotional working memory training. *PLoS One*, *6*, e24372.

Shah, D. A., & Madden, L. (2004). Nonparametric analysis of ordinal data in designed factorial experiments. *Phytopathology*, *94*, 33–43.

Shin, L. M., & Liberzon, I. (2010). The neurocircuitry of fear, stress, and anxiety disorders. *Neuropsychopharmacology*, *35*, 169–191.

Silvert, L., Lepsien, J., Fragopanagos, N., Goolsby, B., Kiss, M., Taylor, J. G., et al. (2007). Influence of attentional demands on the processing of emotional facial expressions in the amygdala. *Neuroimage*, *38*, 357–366.

Sladky, R., Höflich, A., Küblböck, M., Kraus, C., Baldinger, P., Moser, E., et al. (2013). Disrupted effective connectivity between the amygdala and orbitofrontal cortex in social anxiety disorder during emotion discrimination revealed by dynamic causal modeling for fMRI. *Cerebral Cortex*, *25*, 895–903.

Sokolov, A. A., Zeidman, P., Erb, M., Ryvlin, P., Friston, K. J., & Pavlova, M. A. (2018). Structural and effective brain connectivity underlying biological motion detection. *Proceedings of the National Academy of Sciences, U.S.A.*, *115*, E12034–E12042.

Stanislaw, H., & Todorov, N. (1999). Calculation of signal detection theory measures. *Behavior Research Methods, Instruments, & Computers*, *31*, 137–149.

Stephan, K. E., Penny, W. D., Daunizeau, J., Moran, R. J., & Friston, K. J. (2009). Bayesian model selection for group studies. *Neuroimage*, *46*, 1004–1017.

Stephan, K. E., Penny, W. D., Moran, R. J., den Ouden, H. E., Daunizeau, J., & Friston, K. J. (2010). Ten simple rules for dynamic causal modeling. *Neuroimage*, *49*, 3099–3109.

Straube, T., Lipka, J., Sauer, A., Mothes-Lasch, M., & Miltner, W. H. (2011). Amygdala activation to threat under attentional load in individuals with anxiety disorder. *Biology of Mood & Anxiety Disorders*, *1*, 12.

Straube, T., Mentzel, H. J., & Miltner, W. H. (2006). Neural mechanisms of automatic and direct processing of phobogenic stimuli in specific phobia. *Biological Psychiatry*, *59*, 162–170.

Suedfeld, P., & Hare, R. D. (1977). Sensory deprivation in the treatment of snake phobia: Behavioral, self-report, and physiological effects. *Behavior Therapy*, *8*, 240–250.

Van Dillen, L. F., Heslenfeld, D. J., & Koole, S. L. (2009). Tuning down the emotional brain: An fMRI study of the effects of cognitive load on the processing of affective images. *Neuroimage*, *45*, 1212–1219.

von der Malsburg, T. (2015). Saccades: Detection of fixations in eye-tracking data. R package version 0.1-1. https://CRAN.R-project.org/package=saccades.

Vytal, K., Arkin, N., Overstreet, C., Lieberman, L., & Grillon, C. (2016). Induced-anxiety differentially disrupts working memory in generalized anxiety disorder. *BMC Psychiatry*, *16*, 62.

Vytal, K., Cornwell, B., Arkin, N., & Grillon, C. (2012). Describing the interplay between anxiety and cognition: From impaired performance under low cognitive load to reduced anxiety under high load. *Psychophysiology*, *49*, 842–852.